

MICROSTRUCTURE OF ULTRA-HIGH PERFORMANCE CEMENTITIOUS COMPOSITES WITH AND WITHOUT EXCESSIVE SULFATES

ALI H. NAHHAB^{*}, MEHMET GESOĞLU, ERHAN GÜNEYİSİ^{**} and HALIT YAZICI^{***}

^{*}Dept. of Civil Engineering, University of Babylon-Iraq

^{**}Dept. of Civil Engineering, University of Gaziantep, Gaziantep-Turkey

^{***}Dept. of Civil Engineering, University of Dokuz Eylül, İzmir-Turkey

ABSTRACT

Advances in the science of cement-based materials have resulted in the development of a new generation of material, namely ultra-high performance cementitious composite (UHPCC). The primary improvements of UHPCC are achieved by the removal of coarse aggregate, limiting the water-to-binder ratio and introducing micro fine materials such as silica fume.

The present study aimed to investigate the microstructure of UHPCC with and without additional sulfates. For this purpose, two groups of UHPCC were designed at a constant water/binder ratio of 0.174. The first group of UHPCC mixtures was designed with binary blends of Portland cement and silica fume and was reinforced with 2% micro steel fibers by volume. The other group was also designed with binary cementitious blends but without fibers. Each group consisted of five mixes with different SO₃ contents of between 0.11% and 4.5% by weight of natural sand. For each mix, the UHPCC samples were either standard cured or steam cured at 80 °C over a 48 h. Besides, UHPCs were compared to Portland cement mortars. The microstructures of the UHPC were examined using scanning electron microscopy (SEM). Energy dispersive X-ray analysis (EDX) was also performed. SEM observations showed the existence of non-expansive ettringite in the UHPCC samples containing excessive sulfates.

KEYWORDS: Ultra-high performance concrete; Microstructure; Silica fume; steam curing; Sulfates.

1. INTRODUCTION

The basic principles of developing UHPCC are (Richard and Cheyrezy, 1994):

- (1) Replacing coarse aggregates by quartz sands to enhance the homogeneity;
- (2) Improving compacted density by optimizing granular mixture;
- (3) Improving microstructure by applying steam or autoclave treatment;
- (4) Adding micro steel fibers to increase ductility.

When the compressive force is applied, cracks in the paste of ordinary concrete generate from the development of tensile and shear stresses at the aggregate-paste interface. The size of microcracks is directly proportional to the maximum size of aggregate (Richard and Cheyrezy, 1995). Therefore, removing coarse aggregate significantly improves the strength of UHPCC. Another way to enhance the homogeneity is to increase the modulus of elasticity of the paste. For UHPCC, moduli in the range of 55 and 75 GPa can be achieved. This reduces the side effect of

the modulus incompatibility between the paste and aggregate.

The contamination of fine aggregates with sulfates, mostly gypsum is a frequent problem in the Middle East region and similar locations (Kheder and Assi, 2010). In Iraq, for example, it is difficult to find well-graded sand with allowable sulfate content despite the availability of many quarries of natural sands. Due to the scarcity of sulfate-free aggregates, Iraqi code allows only 2.8% SO₃ in ordinary Portland cement, compared to the limits of 3.5% and 3-3.5% which are allowed by British and ASTM specifications, respectively (Al-Rawi et al., 2002).

In the present study, the scanning electron microscopy (SEM) and energy dispersive X-ray analysis (EDX) of UHPCCs and mortars were investigated. For UHPCC, both reference samples and the samples with additional sulfates were investigated. However, for practical reasons, the mortar samples investigated by SEM-EDX were only those made with the highest SO₃ content. Among of many taken and investigated

micrographs and EDX analyses, the typical ones are presented herein.

2. EXPERIMENTAL WORK

2.1. Raw Materials

The cement used in the present study was ordinary Portland cement (CEM I 42.5 R). The specific gravity and specific surface of cement were 3.15 and 394 m²/kg. The silica fume (SF) of 2.2 specific gravity was used also. A type F polycarboxylate-based superplasticizer (SP) was used to provide the desired workability.

The fine aggregate used was natural sand and commercial quartz sand with a specific gravity of 2.66 and 2.65, respectively. The maximum size of the natural sand was 4 mm while the maximum size of quartz sand was chosen as 2.5 mm.

Micro steel fibers with a length of 6 mm and a diameter of 0.16 mm were used to provide fiber reinforcement.

2.2. Mixture Proportioning and sample preparation

Two series of mixtures were produced as shown in **Table 1**. Series A was made with fiber and with binary blends of PC + SF. The mixes of Series B were made without fiber and prepared with binary blends of PC + SF. For each series, five mixes with five different SO₃ contents of 0.11, 0.75, 1.5, 3, and 4.5% by weight of the sand were prepared. Three Portland cement mortar mixes with a w/c ratio of 0.44 were also made with 0.11, 3, and 4.5% SO₃ for the comparison. A Hobart mixer was used for mixing UHPCCs and mortars. The mixtures were poured into the molds and compacted by vibration. After demolding, the samples were subjected to either water curing or steam curing. In the case of water curing, the specimens were stored in water at 22 ± 2 °C until testing. In the case of steam curing, the specimens were kept in water for 24 h and then subjected to heat curing at 80 °C for 48 h at a heating rate of almost 11 °C/min. Thereafter, steam-cured samples were also stored in water at 22 ± 2 °C until the testing age. Actually, denser microstructure can be achieved by using steam curing compared to water curing.

2.3. Testing concrete

In the present study, the microstructures of the UHPCC and mortar mixes were performed by using scanning electron microscopy (SEM). The SEM investigations were performed on small pieces taken from the fractured cubes. This was

done by using JEOL JSM 6390 LV electron microscope with secondary electron (SE). Energy dispersive X-ray analysis (EDX) was also performed. The accelerating voltage was 20 kV for imaging and 15 kV for EDX.

3. RESULTS AND DISCUSSION

3.1 Presence of ettringite

Microscopic observations related to the morphology of ettringite are available in the literature with most of the researches focusing on the heat-induced formation of ettringite (DEF) rather than on the composition-induced formation of ettringite. The differences between the two cases may be the time at which the reaction starts and the mechanism of ettringite formation. While the reaction of composition-induced formation of ettringite initiates at very early ages, the reaction of DEF may take place months or years after exposure to moist environments.

Regarding the mechanism of DEF, it is generally accepted that DEF is a result of reformation of destroyed ettringite in a saturated atmosphere when concrete is subjected to temperatures over 70 °C (**Ramlochan et al., 2003; Heinz and Ludwig, 2004**).

The morphology of ettringite may give valuable information relating to the expansion characteristics of ettringite. The ettringite morphology depends on the available space to fill. In large air voids it takes the shape of needle-like structure. This is non-expansive ettringite (**Divet and Pavoine, 2002**). Massive ettringite may take place in small pores and at the aggregate-cement paste interface. The massive ettringite causes a deleterious expansion (**Tosun and Baradan, 2010**). SEM investigation of UHPCC samples made with excessive sulfates showed the formation of needle-like structures deposited in the air voids as shown in **Figure 1**.

Figure 2 shows the SEM micrographs and EDX analysis of the conventional mortar with 4.5% SO₃ at 28 days of water curing. As seen in the figure, the needle-like crystals of ettringite almost filled the small pore of mortar. This would generate a pressure on the pore walls, thus leading to a deleterious expansion. Furthermore, the expansive ettringite was detected within the paste of the conventional mortars after 180 days of curing in water as seen in **Figures 3**.

In general, contrary to the Portland cement mortars, the massive ettringite was not observed in any of the studied UHPCC samples.

3.2. Presence of Al-Rich Structure

SEM-EDX observations at 180 days confirmed the existence of Al-rich regions in water cured mortar samples with 4.5% SO₃ (mix PC-4.50) and steam cured UHPCC samples, namely PPCSF-3.00 (made with 0.11% SO₃ and PC + SF) as seen in the typical images in **Figures 4**. In other words, the Al-rich structure was present regardless of the matrix type, SO₃ content and curing method. The structure was mainly characterized by high peaks of Si and Al. The Al/Si ratio was 0.653, and 0.372 for mixes PPCSF-3.00 and PC-4.50, respectively. Although the mechanism of the formation of this structure is not clear, it may be the results of the reaction between hydrous silica in the quartz sand and the alumina in cement (**Nahhab, 2015**).

3.3. Presence of Microcracks

Though fracture surfaces may provide useful microstructural information, breaking concrete may develop cracks (**ASTM C1723, 2010**). Therefore, care should be taken in interpretations of cracks. Identifying the materials in the cracks, such as alkali silica gel, ettringite, calcite, or calcium hydroxide can help to determine if cracks are pre- or post-sampling. By examining the microstructure of the fractured samples, it could be observed that the microcracks of UHPCC were empty and so they were post-sampling (**Figure 5**). In other words, these microcracks were attributed to the preparation process rather than to the expansion of the material. On the other hand, the SEM-EDX micrographs of the mortar sample with 4.5% SO₃ at 28 days confirmed the presence of calcium hydroxide (CH) and/or ettringite in the crack (**Figure 6**). This suggested that these cracks were pre-sampling and attributed to the significant expansion which was 0.068% at 28 days.

4. CONCLUSIONS

1. SEM observations showed the presence of non-expansive ettringite in the UHPCC samples which were made with excessive sulfates.
2. Micrographs in the Portland cement mortars contaminated with sulfates revealed the existence of expansive ettringite.
3. Al-rich regions were detected in some of mortar and UHPCC samples.

-

4. By examining the microstructure of the fractured samples, it was observed that the microcracks of UHPCC were empty and so they were post-sampling. On the other hand, the SEM-EDX micrographs of the mortar sample with 4.5% SO₃ at 28 days confirmed the presence of calcium hydroxide and/or ettringite in the crack.

REFERENCES

- Al-Rawi, R. S, Al-Salihi, R. A, Ali, M. H. (2002). Effective sulfate content in concrete ingredients. *Challenges of Concrete Construction, Vol.6, Concrete for Extreme Conditions*. pp. 499–506.
- ASTM C1723 (2010). Standard guide for examination of hardened concrete using scanning electron microscopy. American Society for Testing and Materials. West Conshohocken, PA
- Divet, L., Pavoine, A. (2002). Delayed ettringite formation in massive concrete structures: an account of some studies of degraded bridges. *International RILEM TC 186-ISA workshop on internal sulfate attack and delayed ettringite formation*, Villars, Switzerland. pp. 98–126.
- Heinz, D., Ludwig, H. M. (2004). Heat treatment and the risk of DEF delayed ettringite formation in UHPC. *Proceedings of the international symposium on UHPC*. Kassel, Germany. pp.717-730.
- Kheder, G. F., Assi, D. K. (2010). Limiting total internal sulphates in 15-75 MPa concrete in accordance to its mix proportions. *Materials and Structures*, **43**, 273-281.
- Nahhab, A. H. (2015). Investigating properties of ultra-High Performance cementitious composites made with gypsum-contaminated aggregates. Ph.D. Thesis, University of Gaziantep. Turkey.
- Ramlochan T., Zacarias P., Thomas M.D.A., Hooton R.D. (2003). The effect of pozzolans and slag on the expansion of mortars cured at elevated temperature Part I: Expansive behavior. *Cement and Concrete Research*, **33**, 807-814.
- Richard, P., Cheyrezy, M. (1995). Composition of reactive powder concretes. *Cement and Concrete Research*, **25(7)**, 1501-1511.
- Richard, P., Cheyrezy, M. H. (1994). Reactive powder concretes with high ductility and 200-800 MPa compressive strength. *ACI SP 144-24*, 507–518.
- Tosun, K., Baradan, B. (2010). Effect of ettringite morphology on DEF-related expansion. *Cement and Concrete Composites*, **32**, 271–280.

Table (1): Mix proportions of UHPCCs.

Series	Mix code	SO ₃ % by weight of natural sand	w/b	Material (kg/m ³)							
				PC	SF	1.2-2.5 mm quartz sand	0.6-1.2 mm quartz sand	0-4 mm natural sand	Water	Micro steel fibers	SP
A	FPCSF-0.11	0.11	0.174	824	107	316	250	566	162	143.5	65
	FPCSF-0.75	0.75	0.174	824	107	316	250	566	162	143.5	65
	FPCSF-1.50	1.5	0.174	824	107	316	250	566	162	143.5	65
	FPCSF-3.00	3	0.174	824	107	316	250	566	162	143.5	68
	FPCSF-4.50	4.5	0.174	824	107	316	250	566	162	143.5	71
	B	PPCSF-0.11	0.11	0.174	824	107	341	270	611	162	0
PPCSF-0.75		0.75	0.174	824	107	341	270	611	162	0	50
PPCSF-1.50		1.5	0.174	824	107	341	270	611	162	0	50
PPCSF-3.00		3	0.174	824	107	341	270	611	162	0	52
PPCSF-4.50		4.5	0.174	824	107	341	270	611	162	0	54

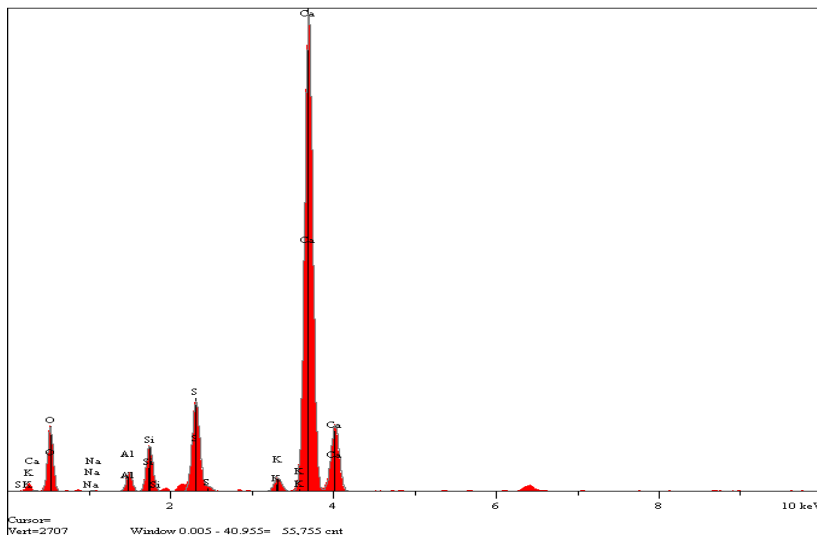
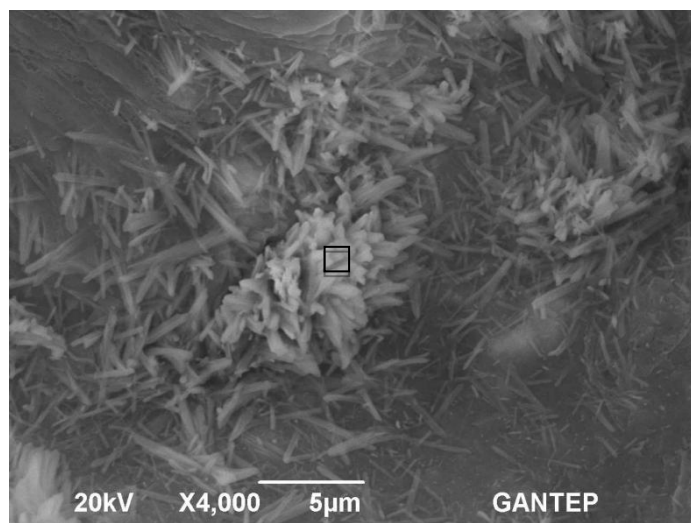
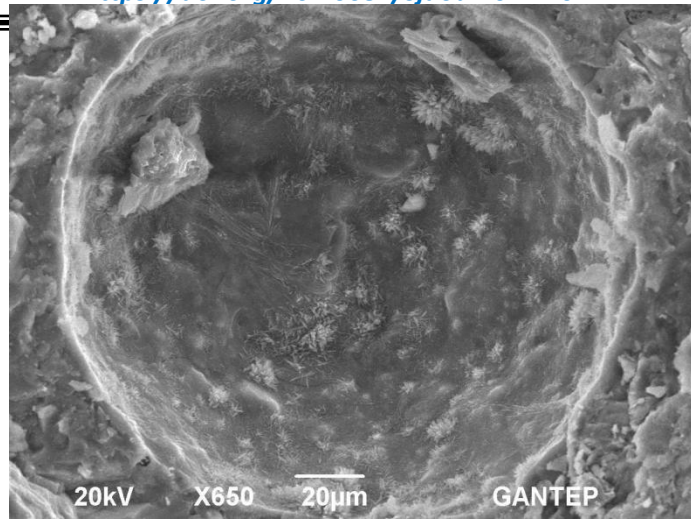


Fig.(1): SEM-EDX analysis of PPCSF-4.50 cured under water.

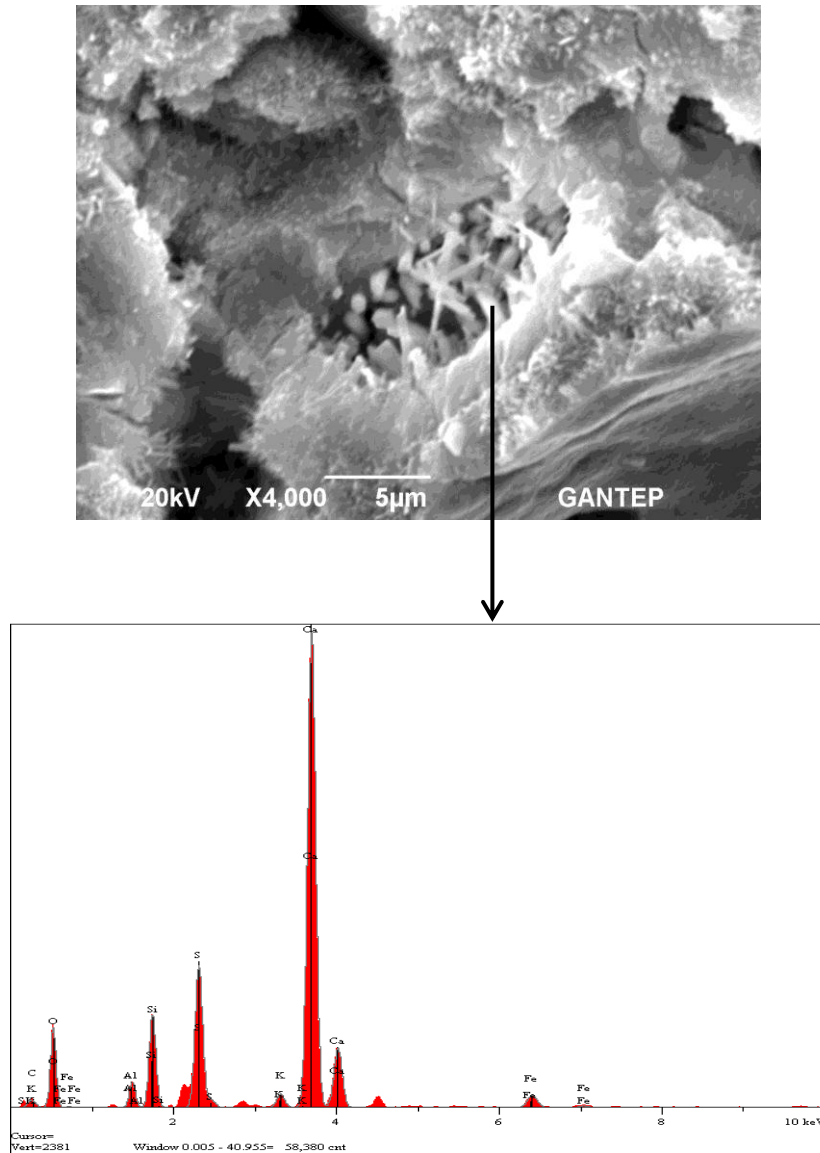


Fig. (2): Needle-like crystals of ettringite filled the small pore of the mortar sample with 4.5% SO_3 after 28 days of water curing.

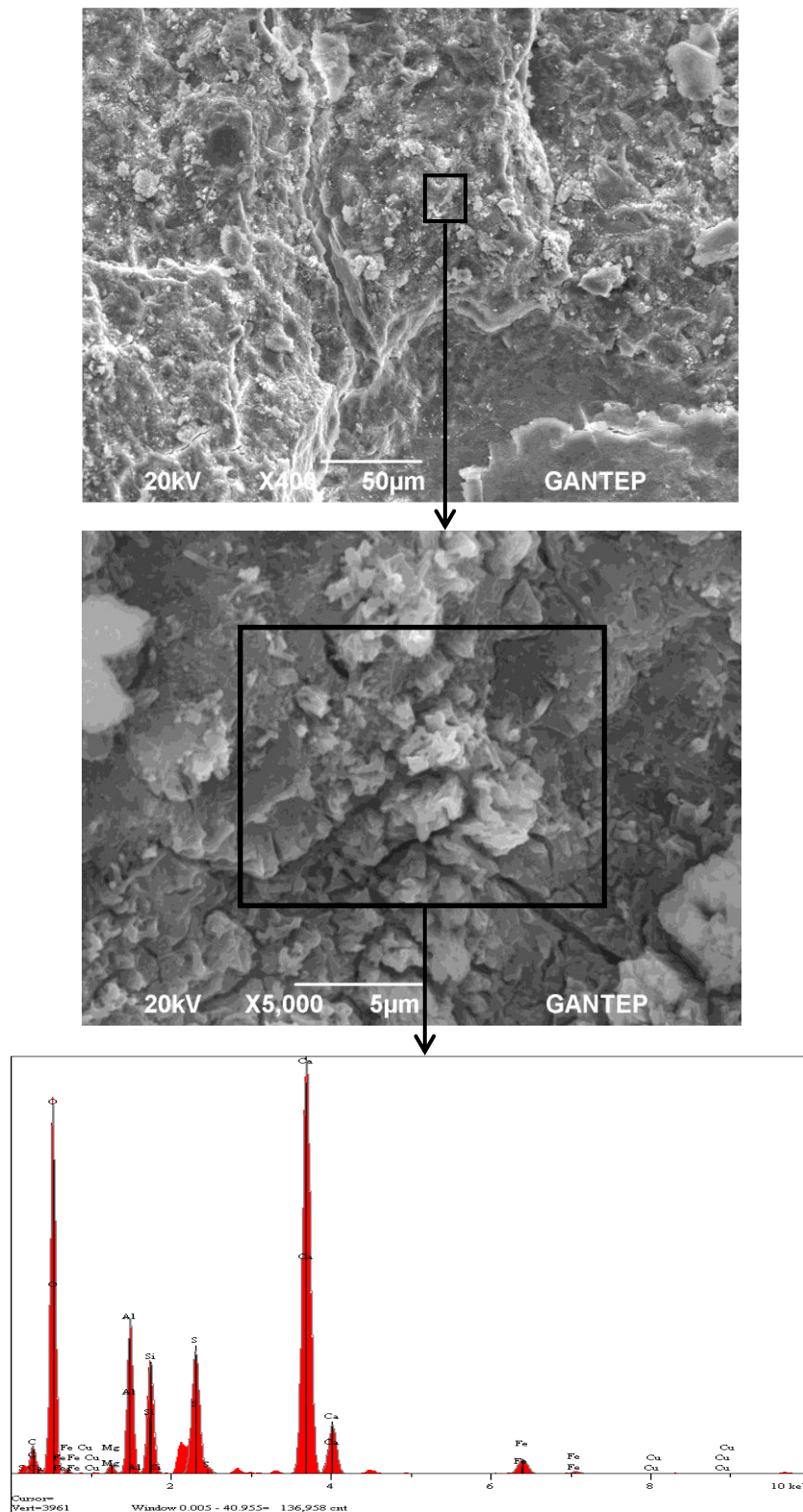


Fig. (3): Expansive ettringite in the cement paste of the mortar sample with 4.5% SO_3 after 180 days of water curing.

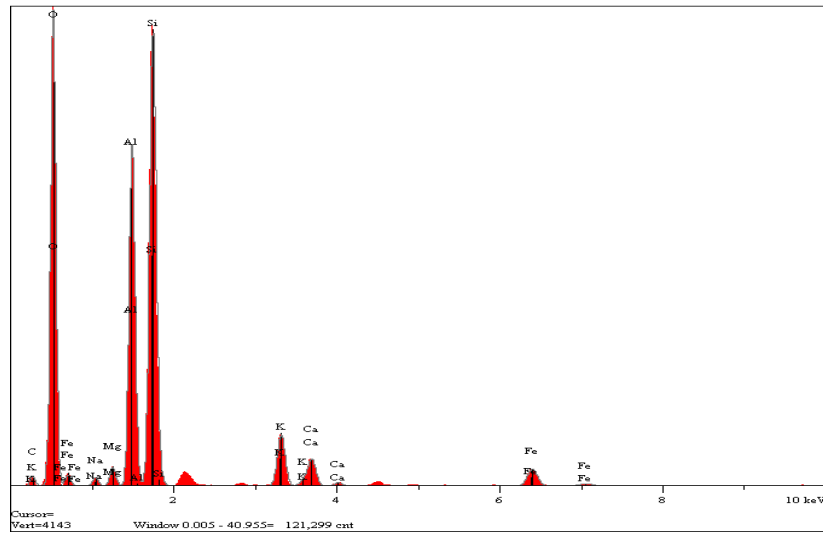
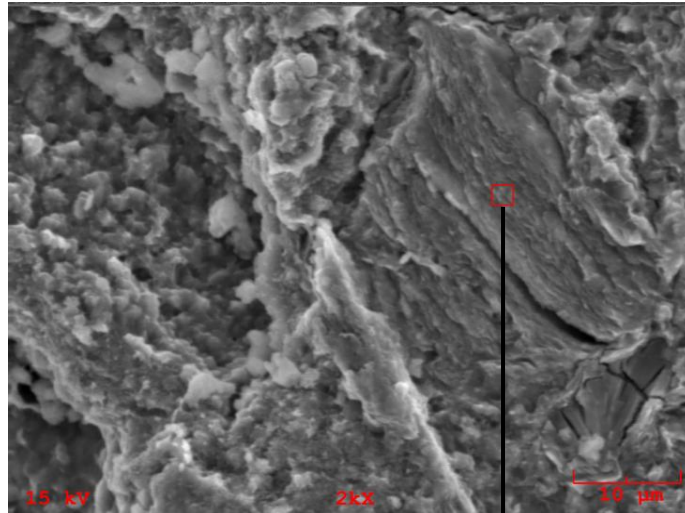


Fig. (4): Al-rich region in steam-cured UHPCC sample PPCSF-3.00

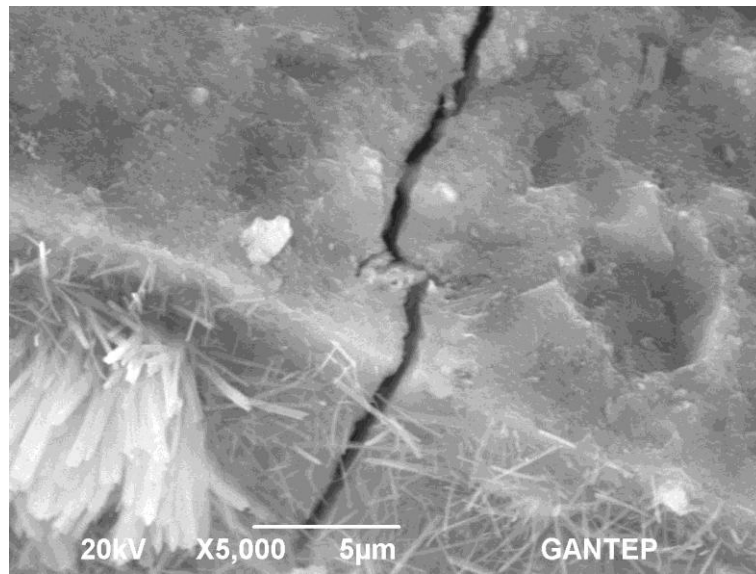


Fig. (5): Empty cracks in UHPCC sample FPCSF-4.50 indicating that the cracks are due to sample preparation

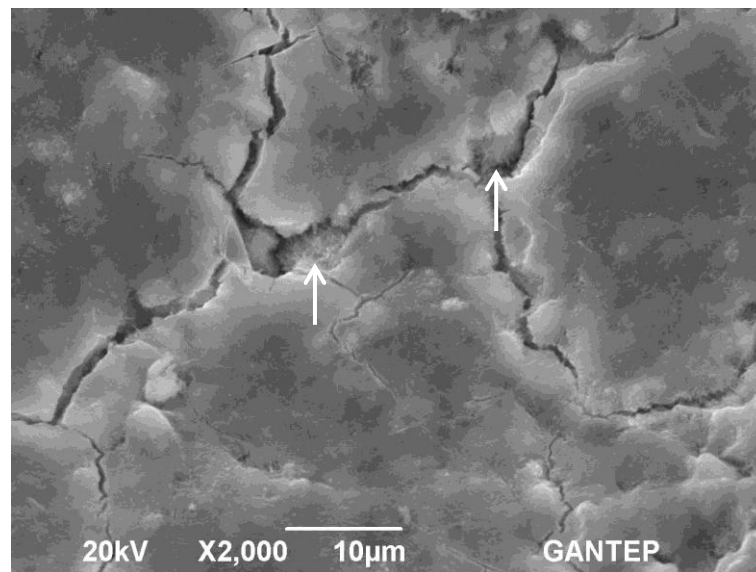


Fig. (6): CH deposited in cracks in mortar sample with 4.5% SO₃ indicating that the cracks are preexisted